Raptor ablation in skeletal muscle decreases Cav1.1 expression and affects the function of the excitation-contraction coupling supramolecular complex

[+]Rubén J. Lopez[+,*]Barbara Mosca, [*]Susan Treves, [+]Marcin Maj, [*]Leda Bergamelli, [#]Juan C. Calderon,[§]C. Florian Bentzinger, [§]Klaas Romanino, [§]Michael N. Hall, [§]Markus A. Rüegg, [†]Osvaldo Delbono, [#]Carlo Caputo and [+,*]Francesco Zorzato

[+]Departments of Anesthesia and of Biomedicine, Basel University Hospital, Hebelstrasse 20, 4031 Basel, Switzerland; [*]Department of Life Sciences, General Pathology section, University of Ferrara, Via Borsari 46, 44100 Ferrara, Italy; [#]Laboratorio de Fisiología Celular, Centro de Biofísica y Bioquímica, Instituto Venezolano de Investigaciones Científicas (IVIC), Apartado 20632, 1020A Caracas, Venezuela; [§]Biozentrum, University of Basel, CH-4056 Basel, Switzerland; [†]Department of Internal Medicine, Section on Gerontology and Geriatric Medicine, Wake Forest University School of Medicine, Winston-Salem, NC 27157, U.S.A.

Short Title: mTOR and excitation-contraction coupling

To whom correspondence should be addressed: Prof. F. Zorzato, Department of Experimental and Diagnostic Medicine, University of Ferrara, Via Borsari 46, 44100 Ferrara, Italy. TEL +39-0532-455356; FAX +39-0532-455351; E-mail zor@unife.it.

Key words: mTOR, excitation-contraction coupling, ryanodine receptor, dihydropyridine receptor, skeletal muscle sarcoplasmic reticulum.

Abbreviation list:, mTOR: mammalian target of rapamycin; RamKO: muscle specific raptor knock-out; EDL: extensor digitorum longus; FDB flexor digitorum brevis, SERCA: sarco(endo)plasmic reticulum calciumATPase; RyR: ryanodine receptor; DHPR: dihydropyridine receptor; GP: glycogen phosphorylase;ECRE: elementary calcium releases events; FWHM: full with at half maximum; FDHM: full duration at half maximum.

SYNOPSIS
The protein mammalian target of rapamycin (mTOR) is a serine/threonine kinase regulating a number of biochemical pathways controlling cell growth. mTOR exists in two complexes termed mTORC1 and mTORC2. Raptor is associated with mTORC1 and is essential for its function. Ablation of Raptor in skeletal muscle results in several phenotypic changes including decreased life expectancy, increased glycogen deposits and alterations of the twitch kinetics of slow fibres. Here we show that in muscle specific raptor knock-out the bulk of glycogen phosphorylase is mainly associated in its cAMP-non stimulated form with sarcoplasmic reticulum membranes. In addition, ^{3}[H]-ryanodine and ^{3}[H]-PN200-110 equilibrium binding show a ryanodine to dihydropyridine receptors ratio of 0.79 and 1.35 for wild type and raptor knock-out skeletal muscle membranes, respectively. Peak amplitude and time to peak of the global calcium transients evoked by supramaximal field stimulation were not different between wild type and raptor knock-out. However, the increase of the voltage sensor-uncoupled RyRs leads to an increase of both frequency and mass of elementary calcium release events (ECRE) induced by hyper-osmotic shock in FDB fibres from raptor knock-out. This study shows that the protein composition and function of the molecular machinery involved in skeletal muscle excitation-contraction coupling is affected by mTORC1 signaling.

SUMMARY STATEMENT (40 words)
A mammalian target of rapamycin (mTOR) is a complex regulating cell growth, proliferation and autophagy. Here show that mTOR complex1 also affects the expression of dihydropyridine receptor, a key component of the supramolecular complex responsible for skeletal muscle excitation-contraction coupling.

INTRODUCTION

The mammalian Target of Rapamycin (mTOR) is a serine/threonine kinase controlling different biochemical pathways activated in response to growth factor and nutrient availability, including protein synthesis, ribosome biogenesis, nutrient transport, lipid synthesis and autophagy, thus playing a central role in metabolism, growth and aging [1-5]. Two different mTOR complexes possessing different roles within the cell have been identified: mTORC1 and mTORC2. The immunosuppressant drug rapamycin is an allosteric inhibitor of mTORC1, a complex playing a role in nutrient sensing and controlling protein synthesis, lipid synthesis and glycolysis [6]. After forming a complex with its cytoplasmic receptor FKBP12 (FK506 binding protein), rapamycin binds mTORC1 and induces its destabilization, resulting in the inability of mTOR to phosphorylate target proteins [6]. mTORC1 complex is made up by mTOR, regulatory associated protein of mTOR (raptor), mammalian LST8/G-protein β-subunit like protein (mLST8/GβL) and PRAS40 [7,8] Its kinase activity is regulated through a dynamic interaction between mTOR and raptor, the latter being a conserved 150-kDa protein, which besides mTOR, also interacts with S6K1 and 4E-BP1. mTORC2 on the other hand, is largely insensitive to rapamycin, is active in growing cells and regulates the actin cytoskeleton, cell survival and apoptosis. It forms a complex with rictor, mSIN1, mLST8 and mTOR [9].

During the past decade, research on the role of mTOR has revealed that this kinase is implicated in a variety of diseases, including cancer, neurodegeneration and metabolic disorders [9]. Furthermore mTOR activity has been shown to be involved in the control of muscle mass and indeed rapamycin treatment delays recovery of skeletal muscle from atrophy while activation of the mTOR's upstream components induces muscle hypertorphy [10]. It has been shown that skeletal muscle specific mTOR inactivation increases the glycogen content of muscle fibres, an effect linked to the down-regulation of glycogen phosphorylase and of other enzymes involved in the glycogenolytic pathway [11]. Similar results were also obtained by Bentzinger et al. who investigated the role of the mTORC1 signalling pathway in skeletal muscle, by generating muscle specific *raptor* KO mice (RamKO)[12]. Skeletal muscles of RamKO mice became progressively atrophic, had increased glycogen content and showed a transition of the metabolic signature from oxidative to glycolitic, despite slow twitch fibre type predominance [12]. Although RamKO mice have poor *in vivo* oxidative muscle performance on the running wheel, *in vitro* tetanic stimulation shows that isolated EDL and soleus from RamKO mice are more resistent to fatigue. The reduction of absolute force development is accounted for by the decrease of muscle mass since after normalisation for cross sectional area there is no significant difference of maximal tetanic force between control and RamKO mice. Nevertheless the twitch kinetics of the soleus from RamKO mice are dramatically affected: there is an increased time to peak and almost doubling of the half relaxation time. Because of these changes and because mTORC1 inhibition is a common therapeutic strategy in humans, we investigated in more detail the functional changes of ablation of mTORC1 in skeletal muscle by examining excitation-contraction (E-C) coupling in RamKO mice. E-C coupling involves the conversion of an electrical signal into a transient increase of the $[Ca^{2+}]$ and is initiated by conformational changes at the level of the L-type voltage dependent calcium channel (DHPR, $Ca_v1.1$) localized in the membrane of the transverse tubules [13,14]. Activation of Ca^{2+} release from terminal cisternae is due to the transmission of a conformational change occurring on the DHPR's, to the ryanodine receptor (RyR1) via direct protein-protein interaction [15-17]. The resulting increase in the intracellular $[Ca^{2+}]$ is due to the opening of the RyR1 and this is followed by Ca^{2+} removal which depends mostly on the activity of sarcoplasmic reticulum calcium pumps (SERCA) localized in the longitudinal sarcoplasmic reticulum, and, to a lesser extent, on the sarcolemmal Na^+/Ca^{2+} exchanger and plasmalemma Ca^{2+} pump [18]. Mutations in the two Ca^{2+} channels (RyR1

and DHPR α1 subunit) directly involved in E-C coupling are the underlying feature of a group of several disorders including core myopathies in which the underlying histological feature is the presence of cores and fibre type I predominance (for review see [19]). Interestingly, the muscles of RamKO mice also exhibit core-like structures and slow fibre type predominance [12].

In the present study we investigated the functional and biochemical properties of the sarcoplasmic reticulum (SR) membranes from RamKO mice. We found that the inactivation of mTORC1 is associated with the compartmentalization of glycogen phosphorylase to sarcoplasmic reticulum membranes. In addition, we found an increase of the: i) half-time of the decay of the calcium transient in soleus fibres; ii) ryanodine to dihydropyridine receptors ratio; iii) frequency and mass of elementary calcium release events (ECRE) induced by hyperosmotic shock in FBD fibres. Altogether our data suggest that protein composition and function of the membrane compartments involved excitation-contraction coupling is affected by mTORC1 signalling.

MATERIALS AND METHODS

RamKO mice: details of the targeting strategy and initial characterization of RamKO mice are previously described [12]. Knockout mice were identified by PCR amplification of genomic DNA. All experiments were conducted on male mice in accordance with local Kantonal guidelines and regulations (Kantonales Veterinäramt Basel Stadt).

RNA extraction, reverse transcription and PCR reactions: Total RNA was extracted from mouse leg muscles using Tri-reagent following the manufacturer's recommendations (molecular Research Centre). Total RNA was converted into cDNA using SuperScript$^{(TM)}$ II Reverse Transcriptase (Invitrogen) as previously described [20]. PCR reactions were carried out using the following primer sets: Mouse β-actin Forward: 5'-GGACCTGACAGACTACCTCA-3' and Reverse 5' GCAGTAATCTCCTTCTGCAT-3'; DHPRα1 ($Ca_v1.1$) Forward 5' –CATTAGGTAGAGCCGTGCACCTG-3' and Reverse 5'-GCCTGTTGTCATGACGAAGTTAGC- 3'. Amplification conditions were 5 min at 95°C followed by 35 cycles of 30 s denaturation at 92°C, 40 s annealing at the recommended temperature for each primer pair and 40 s extension at 72°C followed by a final extension for 5 min at 72°C using the 2.5x Master Mix Taq polymerase from Eppendorf. The products of the PCR reaction were separated on a 1% agarose gel, and the DNA bands were visualized by ethidium bromide staining.

SR isolation, Western blotting and biochemical assays: Total SR was prepared as previously described from mouse skeletal muscle [20]; vesicles enriched in terminal cisteranae, longitudinal sarcoplasmic reticulum and plasmalemma were prepared as described by Saito et al. [21] and stored in liquid nitrogen until used. C_2C_{12} myotubes were treated for 16 hours with 20 μM rapamycin or left untreated; cells were then washed twice with PBS, harvested and the heavy SR protein fraction was obtained by differential centrifugation. For Western blotting, proteins were separated by SDS PAGE, blotted onto nitrocellulose and probed with commercial antibodies against SR proteins (SERCA1, SERCA 2, calsequestrin, calreticulin, sarcalumenin, RyR1, DHPRα1, DHPR ß1, albumin, SRP-35 or anti-JP-45 antibodies [20] followed by peroxidase conjugated secondary antibodies. The immunopositive bands were visualized by chemiluminescence as previously described [22]. To accurately quantify DHPR and RyR content in the SR, and the Ca^{2+} dependency of [^{3}H]ryanodine binding, radioligand binding experiments using [^{3}H] PN200-110 (DHPR expression) and [^{3}H]ryanodine were performed as described [23]. The different free Ca^{2+} concentrations (750 pM, 9.1 nM, 95 nM, 1.1 μM, 9 μM, 104 μM, 1 mM) were obtained by the addition of different amounts of $CaCl_2$ as described by Fabiato [24]. The amount of bound [^{3}H] ligand was measured by liquid scintillation counting.

***In Vitro* Muscle Strength Assessment:** To test force in vitro, EDL and soleus muscles were dissected and mounted into a muscle testing setup (Heidelberg Scientific Instruments). Muscles were stimulated with 15-V pulses for 0.5 ms, and force was digitized at 4 kHz by using an AD Instruments converter. EDL tetanus was recorded in response to a 400 ms train of pulses delivered at 10–120 Hz; soleus, tetanus was recorded in response to an 1100 ms train of pulses delivered at 10–150 Hz . Specific force was normalized to the muscle cross-sectional area [CSA] per wet weight (mg)/length (mm) per 1.06 (density mg/mm^3) as previously described [23].

Isolation of Extensor Digitorum Longus (EDL) and soleus muscle fibres: Single muscle fibres were obtained from 6-8 weeks old mouse hindlimbs by enzymatic dissociated, as previously described [25]. Briefly, muscles were dissected and pinned via the tendons to a

Sylgard-lined dissecting chamber. The outer connective tissue was removed, and the muscles were incubated in Tyrode's solution containing 0.22% Type I collagenase (Sigma) at 37°C for 1 h followed by rinsing in 10% foetal bovine serum in DMEM. To release single fibres, muscles were triturated gently in serum free DMEM, then plated on glass coverslips pre- treated for 2 hours with 1.5 µl of natural mouse laminin (Invitrogen) diluted with distilled water. Fibres were then incubated in DMEM 10% foetal bovine serum, 1% Penicillin/Streptomycin, 5% CO_2 at 37°C overnight. FDF fibers were isolated as previously described [23].

Calcium measurements: The resting Ca^{2+} concentration was monitored in isolated fibres from RamKO mice and control littermates with the ratiometric fluorescent Ca^{2+}indicator indo-1/AM; changes in the $[Ca^{2+}]_i$ induced by electrical depolarization were monitored in EDL and soleus fibres loaded with Mag-Fluo-4/AM in Tyrode's buffer. All experiments were carried out at room temperature (20-22°C) in the presence of 50 µM N-benzyl-p-toluensulfonamide (BTS) (Tocris) to minimize movement artefacts. Measurements were carried out with a Nikon ECLIPSE TE2000-U inverted fluorescent microscope equipped with a 20x PH1 DL magnification objective. The light signals from a spot of 1 mm diameter of the magnified image of FDB fibres, were converted into electrical signals by a photomultiplier connected to a Nikon Photometer P101 amplifier. Calcium transients were collected by custom made (RCS AUTOLAB) software and analyzed by PowerLab Chart5 and Origin.6 programs. Changes in fluorescence were calculated as ΔF/F = (Fmax-Frest)/(Frest).
FDB fibres were isolated, kept for 4 hr in a 37°C 5% CO_2 cell incubator, placed in a laminin coated coverslip and loaded for 20 min at room temperature with 10 µM fluo-4 AM Ca^{2+} indicator (fluo-4 AM, Molecular Probes, Eugene, OR, USA). All experiments were performed at room temperature.. ECREs were measured using a Nikon A1R laser scanning confocal microscope (Nikon Instruments Inc. Melville, USA) with a 60X oil immersion Plan Apo VC Nikon objetive, numerical aperture 1.4. (Nikon Instruments Inc. Melville, USA). 5 sec duration linescan images (x,t) were acquired in resonant mode at 7680 lps with 512 pixels (0.05 µm/pixel) in the x- and 39936 pixels (0.126 ms/pixel) in the t-direction using a pinhole size of 72.27 µm. Fifteen images were taken at different positions across each cell. The Ca^{2+} indicator was excited with a laser at 487 nm and the fluorescence emitted at 525+/-25 nm was recorded. To minimize photo damage, the laser intensity was set at 3~4 % of the maximal power. The viability of fibres after osmotic shock was assessed by monitoring single calcium transient evoked by supramaximal field stimulation pulses. Fibres were first perfused with isotonic (~290 mOsm) Normal Ringer (NR) (in mM, 140 NaCl; 2 $MgCl_2$; 2.5 $CaCl_2$; 10 HEPES; 5 KCl; pH adjusted to 7.4) using a Minipuls 2 peristaltic pump (Gilson Medical Electronics, France). To induce ECREs cells were perfused with a Hypertonic solution (~420 mOsm) by increasing the Ca^{2+} concentration to 50 mM the (in mM, 140 NaCl; 2 $MgCl_2$; 50 $CaCl_2$; 10 HEPES; 5 KCl; pH adjusted to 7.4) [26, 27]. Osmolarity of the solution was assessed with a Vogel 801 Osmometer (Vogel GmbH, Gießen, Germany). All solution contained 10 µM BTS.

ECRE analysis
ECREs morphology (amplitude, ΔF/F0; full width at half-maximum amplitude, FWHM, full duration at half-maximum amplitude FDHM) were determined from linescan images using the open source image analyser software Fiji [28]. After images were binned by average 4x at the *t* axis, they were processed using the automated spark detection plugin Sparkmaster [29]. Because of the heterogeneity of the ECREs duration, events were split in two groups: the short lasting events with less than 50 ms of FWHM and the long lasting events ECREs with >50 ms of FWHM duration [30]. Frequency was calculated for each group by counting

the number of events occurring per image. The mass was determined by the following formula mass= 1.206* $\Delta F/F0*FWHM^3$ [31]. Statistical analysis was performed using the program OriginPro® version 8.6.0 (Northampton, MA). ECRE derived from 25 and 26 fibres obtained from 5 WT and RamKO mice, respectively. Data is expressed as mean ± SEM; values were considered statistically significant if $P<0.05$ using the Student's *t*-test.

Glycogen phosphorylase activity measurement: Glycogen phosphorylase activity was measured as described [32-34]. Reactions were initiated by adding 30-60 µg of SR to a 500 µl of reaction buffer containing 50 mM imidazole pH 7.0, 20 mM K_2HPO_4, 1.25 mM $MgCl_2$, 5 µM glucose 1,6-diphosphate, 0.5 mM DTT, 3 µg/ml phosphoglucomutase, 0.25% BSA, 10 mg/ml AMP-free glycogen. For measurement of total activity (forms "a" and "b") AMP was added to obtain a final concentration of 3 mmol/l. The reaction was carried out at 30°C for 30 min (total activity), or for 60 min (to determine the mount of form "a") and terminated by the addition of 60 µl 0.5 M HCl. Aliquots of 50 or 100 µl (for total and form "a" measurement, respectively) of primary reaction were added to 1 ml of a glucose-6-phosphate dehydrogenase reaction buffer containing 50 mM Tris-HCl, pH 8.0, 1 mM EDTA, 250 µM NADP and 0.5 µg/ml glucose-6-phosphate dehydrogenase. This reaction was allowed to proceed for 10 min at room temperature and the absorbance at 340 nm of the samples was determined spectrophotometrically to quantify the degree of conversion of NADP to NADPH (which is proportional to the content of glucose 6-phosphate formed in the first reaction). Glycogen phosphorylase activity is expressed in micromoles per minute per milligram protein (U/mg).

Luciferase reporter assay: The constructs containing DHPRα1.1 promoter region fragments (Luc7P-724, Luc/P756) were cloned in frame in pGL3-basic expression vector (Promega)[35]. C_2C_{12} myoblasts ($2x10^4$ cells per dish) were plated on gelatin-coated 35 mm cell culture dishes and allowed to grow in DMEM plus Glutamax, 4.5 g/l glucose, 20% foetal bovine serum, 50 units/ml penicillin, 50 µg/ml streptomycin until 50% confluent. Two µg of each construct and 200 ng of the control vector pRL-TK were used for transfection using the FuGENE6 transfection reagent (Roche). Twenty four hours after transfection cells were induced to differentiate by changing the medium to DMEM plus Glutamax, 4.5 g/l glucose, 5% horse serum and penicillin/streptomycin. After 4-6 days, when cells had visibly fused into mytoubes, 20 µM Rapamycin (Sigma) was added as described [36, 37]. Cells were then washed twice with PBS and lysed using Passive Lysis Buffer (Promega). Firefly Luciferase and Renilla activity were measured with $Victor^2$ Luminometer (PerkinElmer). Firefly Luciferase activity was normalized to Renilla activity and expressed as mean (± S.E.M) enzymatic activity units.

RESULTS

Mechanical properties of isolated fibres and content of proteins involved in excitation-contraction coupling in skeletal muscles of RamKO mice

Ablation of raptor induces changes of the mechanical properties of fast and slow twitch muscles [12]; figure 1 shows representative traces of twitch and tetanic force of EDL and soleus from control and RamKO mice [12]. Although tetanic specific force in EDL and soleus muscles do not vary between control and RamKO [12] mice, the twitch kinetics in RamKO soleus show a remarkable prolongation of the half relaxation time at lower peak force. The changes of the mechanical properties of the twitch in EDL and soleus muscles could be due (i) to fibre-type switching induced by ablation of Raptor, (ii) to an effect on the contractile protein machinery, (iii) to alterations of the E-C coupling mechanism, or (iv) to a combination of two or more of these mechanisms.

Protein composition of skeletal muscle sarcoplasmic reticulum from RamKO mice

Analysis of the main protein components of total sarcoplasmic reticulum membranes from RamKO mice and control littermates revealed no significant changes in the content of SERCA1, SERCA2, JP-45, calsequestrin and calreticulin. While there was a small but significant decrease in sarcalumenin (Fig. 2), a modulator of SERCA activity [38]. We also found a decrease of SRP35, a newly identified membrane-bound retinol dehydrogenase of sarcotubular membranes [22].

RamKO ablation affects the excitation-contraction coupling macromolecular complex

To study in greater detail the effect of raptor ablation, we determined the membrane density of the two core components of the E-C coupling machinery, namely the $Ca_v1.1$ ($\alpha 1.1$ of the DHPR) and RyR1 by performing quantitative Western blot analysis and equilibrium ligand binding on the crude microsomal preparation isolated from skeletal muscle of RamKO and control littermates. The most interesting results of this study are that the content of $Ca_v1.1$ in RamKO mice was reduced by almost 50% compared to control littermates (Fig. 3A). Equilibrium binding of the $Ca_v1.1$ ligand PN200-100 to crude SR membranes shows that the Bmax for PN200-100 binding was 0.68±0.05 and 1.25±0-13 pmoles/mg protein in RamKO and control littermates, respectively, with no significant changes of its dissociation constant (K_d = 0.96 ± 0.16 vs.1.35 ± 0.32 nM, mean ± S.E.M., *n* = 6 for RamKO and control littermates, respectively). The reduced expression of Cav1.1 is, surprisingly, accompanied by a 3.5 fold increase of the content of the Cavß1 subunit (Fig. 3B and C). On the other hand, the decrease in the total amount of $Ca_v1.1$ was not due to a reduction of the relative amount in T-tubule membranes in the total sarcotubular membrane fraction, as the content of albumin, a marker for T-tubules [39] was unchanged (Fig. 3B and C and Fig. 4B). mTORC1 regulates protein expression by affecting translation via S6K1 and 4E-BP [5], and/or by controlling the transcription of several additional genes [40]. To determine if the decrease in $Ca_v1.1$ in the muscles of RamKO mice was due to alterations in transcription we performed semi-quantitative PCR experiments. As shown in Fig. 4A there were no significant changes in $Ca_v1.1$ mRNA content in RamKO mice. We next evaluated the activity of the $Ca_v1.1$ promoter in C_2C_{12} myotubes and HEK293 cells transfected with a luciferase reporter construct containing the 5' flanking region of the $Ca_v1.1$ gene. Figure 4C shows that the $Ca_v1.1$ promoter is active in C_2C_{12} myotubes but not in HEK293 cells. Since FKBP12 is a ubiquitously expressed protein, including in C2C12 myotubes [41], we next tested the effect of rapamycin, a drug which pharmacologically mimics the effect of knocking out raptor, on the activity of the Cav1.1 promoter. Incubation of C2C12 myotubes for 2 and 16 hours with 20 μM rapamycin abolished the phosphorylation of the mTORC1 downstream target S6 ribosomal protein (Fig. 4D), without influencing the activity of the $Ca_v1.1$ promoter (Fig. 4C). Nevertheless, rapamycin treatment of C2C12 myotubes causes a

decrease of the immunoreactive band corresponding to the $Ca_v1.1$ (Fig.4E) without effecting calreticulin (CR) content, an extrinsic protein of the sarcoplasmic reticulum membrane. Our data clearly show that, even in the presence of a partial inhibition of the mTORC1 complex [42], the phenotype of rapamycin treated C2C12 cells recapitulate the effect of Cav1.1 expression that observed in RamKO mature skeletal muscle fibres. In particular, it appears that functional ablation of mTORC1 affects the synthesis and/or the stability of $Ca_v1.1$. A great deal of data show that rapamycin dissociats FKBP12 from the RyR complex leading to leaky RyRs [43]. It is unlikely that the decrease of the Cav1.1 expression results from the acute appearance of leaky RyR in C2C12 cells, since chronic disregulation of intracellular calcium concentration in muscle fibres expressing leaky RyR1 mutation do not display a decrease of Cav1.1 current density [44]. The decrease of the total sarcotubular membrane density of $Ca_v1.1$ was apparently also not paralleled by a decrease of the sarcoplasmic reticulum RyR1 calcium release channels as we found no change in the Bmax of equilibrium [^{3}H]-ryanodine binding to the total SR membrane fraction (0.99 +/0.1 vs 0.92+/- pmol/mg pr for WT and RamKO, respectively) (Fig. 5) from RamKO and control littermates.

Glycogen phosphorylase is targeted to sarcoplasmic reticulum membrane in skeletal muscle from RamKO mice

Skeletal muscles from RamKO and control littermates were homogenized and fractionated by differential centrifugation. Comparison of the protein profile of total homogenates, shows a decrease of a band of 97 kDa in the total homogenate of skeletal muscle from RamKO mice compared to that from control littermates (*). It was previously shown that skeletal muscle specific mTORC1 inactivation reduces the content of glycogen phosphorylase, a result consistent with glycogen accumulation in RamKO muscle fibres [11, 12]. Nevertheless, SDS gel electrophoresis of isolated SR membrane fractions revealed that the band with an apparent molecular mass of 97 kDa was enriched in the total SR of RamKO mice (Fig. 6A). Mass spectroscopy identified the 97 kDa sarcoplasmic reticulum protein band as the glycogen phosphorylase (GP). This finding was further confirmed by staining western blot of total SR membrane proteins with specific anti-glycogen phosphorylase antibodies (Fig. 6D). Quantification showed that ablation of raptor led to a 2.9 fold increase of glycogen phosphorylase associated with the total SR membrane fraction (Fig. 6B). Subfractionation of SR membranes by sucrose density centrifugation revealed that glycogen phosphorylase was enriched in the light R1 fraction (Fig. 6C; white arrowheads), which is made up of membranes derived from longitudinal SR, sarcolemma and T tubules. Glycogen phosphorylase activity is regulated in several ways including (i) substrate availability, (ii) interconversion (phosphorylation/dephosphorylation) and (iii) allosteric modification, with AMP being a key activator [45, 46]. We assessed whether the cAMP-stimulated (GP-a) or cAMP non-stimulated (GP-b) forms of the enzyme are enriched in the muscle from RamKO mice; as shown in Figure 6E, there was a similar increase in GP-total and GP-b activity, suggesting that the cyclic AMP-non-stimulated form of glycogen phosphorylase is enriched in the SR membranes of RamKO mice [47]**.** Hirata et al. reported that GP is a negative regulator of RyR since it decreases mastoparan induced calcium release [48], and thus may affect the twitch kinetics. To explore this possibility, we studied Ca^{2+} homeostasis in enzymatically dissociated single EDL and soleus fibres.

Calcium transients on isolated EDL and Soleus fibres

To assess the resting calcium concentration we loaded EDL and soleus fibres with the ratiometric fluorescent Ca^{2+} indicator Indo-1. In both WT and RamKO mice the resting [Ca^{2+}] in EDL fibres from control mice is slightly higher compared to that in soleus fibres. On the other hand EDL and soleus fibres from RamKO mice exhibited a small but

significant decrease of the resting [Ca^{2+}] compared to control littermates (Table 1). Mag-Fluo-4 a low affinity calcium indicator was used to monitor rapid Ca^{2+} transients (Fig. 7) elicited by an action potential in single EDL and soleus fibres excited by supramaximal field stimulation [49]. The results we obtained are summarized in Table I. The ΔF/F peak Ca^{2+} transient amplitude in EDL from WT (0.46± 0.04, mean ±S.E.M. n=29 fibres) mice was 18% and 22% higher compared to that of soleus muscles from WT (0.38±0.02, mean ± S.E.M. n= 22 fibres) and RamKO (0.36 ±0.02, mean ±S.E.M. n= 5 fibres) mice, respectively. Surprisingly, the peak amplitude and the 10-90% rise time of the calcium transients were not different between RamKO mice and control littermates both in EDL and soleus. The 10-90% fall time of the calcium transients in soleus from RamKO mice is increased compared to that of WT (120.2 ±15.7, n=25 vs 66.2±7.4, n=22 fibres, respectively; values are mean ±S.E.M.; $p<0.05$ Mann Whitney test). The 10-90% fall time of the calcium transients reflect the removal of calcium from the cytosol leading to muscle relaxation. Slow fibres are distinct from fast fibres since they typically display a lower relaxation rate compared to fast fibres [50]. In addition, peak calcium release induced by an action potential is lower in slow fibres compared to fast fibres [51]. The increase of 10-90% fall time and the decrease of ΔF/F peak Ca^{2+} transient are consistent with the observation that almost 100% of the fibres of the soleus from RamKO mice are of type 1 [12]. EDL fibres from RamKO mice exhibited a small and not- significant increase of 10-90% fall time of the calcium transients. Similar results were also obtained with enzymatically dissociated FDB fibres (not shown).

The lack of a decrease of the peak amplitude calcium transients evoked by an action potential in RamKO EDL and soleus fibres is apparently inconsistent with the decrease of density of $Ca_v1.1$ in the T tubular membrane. A number of possibilities may account for this discrepancy. For example, the 50% decrease of $Ca_v1.1$ in RamKO fibres ought to be accompanied with a larger fraction of voltage-sensor uncoupled RyR1. It has been proposed that (i) the interaction of $Ca_v1.1$ with RyR1 inhibits the appearance of elementary calcium release events (ECRE) in mammalian adult muscle fibres [26, 50], and that (ii) the global calcium transients supporting EC coupling in skeletal muscle fibres may result from the summation of ECRE [30]. Equilibrium binding on total microsomes shows that in RamKO there are five/six uncoupled RyRs per voltage-sensor coupled RyR, while in WT there is one/two uncoupled RyR per voltage-sensor coupled RyR. On the basis of the equilibrium ligand–binding data we reasoned that the doubling of the voltage-sensor uncoupled RyRs may affect ECRE. If this were so, the release of calcium from voltage-coupled RyRs in RamKO fibres might propagate to adjacent voltage-sensor uncoupled RyRs triggering a larger number of ECRE, which together contribute to the global amplitude of the peak calcium transients in muscle fibres from RamKO. In the next set of experiments, we set out to test this idea by measuring the ECRE properties in FDB fibres from WT and RamKO mice induced by hyperosmotic shock [26, 27], a treatment that weakness the inhibitory activity of $Cav_{1.1}$ on the RyR1, and thus unmasks the spontaneous activity of RyR1.

Elementary Calcium Release Events (ECRE) in WT and RamKO FBD fibres

Intact single FDB fibres from WT and RamKO mice were first perfused with normal Ringer solution, and then they exposed to hyperosmotic Ringer solution containing 50 mM $CaCl_2$ [26, 27]. After exposure to hyperosmotic solution the FDB fibres were rinsed with normal Ringer and their viability was confirmed by their ability to respond with a robust global calcium transient upon the delivery of an action potential by supramaximal field stimulation (Fig1S). The perfusion of FDB fibres from WT and RamKO with normal Ringer solution did not cause the appearance of spontaneous elementary calcium release events (ECRE)(Fig. 8A, C, D and F left panels). Exposure to hyperosmotic Ringer solution solution containing 50 mM $CaCl_2$ [26, 27], induced localised increase of Fluo-4 fluorescence signals,

which were mostly distributed under inner leaflet of the sarcolemma (Fig. 8 B and E, Supplementary videos). Reperfusion of FDB fibres with normal Ringer abolished the appearance of local transient increases of Fluo-4 fluorescence (Fig. 8C and Fig.8F). Fig. 8H and Fig. 8I show x,t line scan images of fibre exposed to hyperosmotic solution. As can be seen hyperosmotic treatment causes transient increase of the fluorescence, and on the basis of the criteria proposed by Kirsch et al. [30], we refer to the local increase of Fluo4 fluorescence as elementary calcium release events (ECRE). ECRE analysis was performed with Sparkmaster plug-in, and ECRE were divided into two groups: short lasting (sparks-like) events having a FDHM lower than 50 ms and long lasting (ember-like) events FDHM higher than 50 ms [29]. Analysis of 1923 and 2547 short lasting ECRE from WT and RamKO fibres revealed significant differences of the morphological parameters of ECRE. Although the amplitude of short lasting ECRE was not different between WT and RamKO FDB fibres, the latter fibres exhibited a 10% increase of both FWHM (0.89 ± 0.01 vs 0.98± 0.01 μm for WT and RamKO FDB fibres, respectively; $P<0.05$) and FDHM (13.31 ± 0.26 vs 14.11±0.24 ms for WT and RamKO FDB fibres, respectively; $P<0.05$). The estimated ECRE mass at peak time of the ΔF/F was 37% increased in RamKO FDB fibres (0.62± 0.02 vs 0.85± 0.03 μm^3 for WT and RamKO FDB fibres, respectively; $P<0.05$). The increase of estimated ECRE mass was paralleled by a 30% increase of the frequency of short lasting ECRE events in RamKO fibre (6.81±0.36 vs 8.83±0.40 sparks/image for WT and RamKO FDB fibres, respectively; $P<0.05$). The appearance of ECRE in both WT and RamKO fibres dropped to zero upon preincubation of the fibres with RyR, indicating that the calcium source flux of ECRE are the RyR calcium release channels (Fig. 8 J and Fig8 K).

DISCUSSION

In this study we investigated the structural and functional properties of the membrane compartment involved in excitation-contraction coupling of skeletal muscle from WT and Raptor KO mice. Our results show that muscle specific ablation of Raptor and the consequent downregulation of the mTORC1 complex, causes a 1.70 fold increase of the RyR1 to dihydropyridine receptors ratio in total sarcotubular membranes. This event increases both the frequency and width of elementary calcium release events (ECRE) induced by exposure of FDB fibres to hyperosmotic shock. In addition, in RamKO skeletal muscles, the cAMP non-stimulated form b of glycogen phosphorylase is mostly associated with the sarcotubular membrane fraction. We propose that mTORC1 signalling affects the structure and function of the membrane compartments involved in excitation-contraction and excitation-glycogen metabolism coupling.

$Ca_v1.1$ content in RamKO mice

The transmission of the signal from the T tubular membrane to the sarcopalsmic reticulum is performed by a supramolecular complex in the contact region between the two membrane systems. The core components of such a complex are the $alpha_1$-subunit ($Ca_v1.1$) of the L-type Ca^{2+} channel dihydropyridine receptor (DHPR), the ryanodine receptor (RyR) and calsequestrin which serve as voltage sensor, SR Ca^{2+} release channel, and calcium storage protein, respectively [13]. The decrease of the membrane density of DHPR is not accompanied by a decrease of the membrane density of the RyR1 whereby the ryanodine to dihydropyridine receptors ratio of RamKO mice is higher compared to that of WT mice. The lower membrane density of the DHPR is not due to mis-localization of the protein to a different membrane compartment as the total amount of $Ca_v1.1$ was also reduced in the total muscle homogenate, nor due to decreased levels of specific transcript. A similar decrease of the membrane density of DHPR was previously reported by Avila and Dirksen [37] upon acute treatment of cultured myotubes with 20 μM rapamycin and confirmed in the present study in C_2C_{12} cells treated in culture with rapamycin. However, it seems that the functional effect caused by the decreased membrane density of DHPR depends on the maturation stage of muscle cells, namely in myotubes [37] it causes a substantial decrease of the voltage-depenent calcium release, while in mature RamKO FDB fibres (this work) calcium release evoked by action potential is not affected. The decrease in DHPR content may be caused by increased degradation via ubiquitination and indeed it has been shown that rapamycin treatment induces protein ubiquitination in rat myocardium and mTOR inhibition induces autophagy [53, 54]. Interestingly, the ratio of DHPR to RyR1 in slow fibers is lower compared to that in fast fibers, leading to a higher content of uncoupled RyR1 in soleus compared to fast twitch muscles [55]. Thus, our equilibrium binding results are consistent with the fast to slow fiber transition in RamKO muscles [12], in particular more than 90% of soleus's fibres from RamKO are of type 1. Importantly however, while this reduction in voltage sensor does not seem to be directly responsible for changes in E-C coupling, it may trigger some of the structural variations seen on biopsied muscles, particularly the presence of smaller fibres containing core-like structures such as those described in the mouse RamKO muscles [12]. Indeed, immunofluorescence analysis of skeletal muscle biopsies from some patients with recessive *RYR1* mutations show that mis-alignment of RyR1 and DHPR is a feature of some patients with core myopathies [56]. A decrease of the DHPR calcium channels has also been reported in myotubular/centronuclear myopathy [57, 58]. Razidlo et al. [59] proposed that the lack of myotubularin inhibits Akt signalling to mTORC1 leading to down-regulation of the signalling pathways mediated by the mTORC1 complex.

RyR/ $Ca_v1.1$ ratio in skeletal muscle of RamKO mice.

High resolution electron microscopy has demonstrated that $Ca_v1.1$ are organised in groups made up of four units regularly oriented in the T- tubular membrane to form structures referred to as tetrads, which correspond to the position of every other RyR localised in the opposite SR terminal cisternae membrane [14]. Equilibrium binding with total sarcotubular membrane fractions show a ryanodine to dihydropyridine receptor ratio of 0.79 and 1.35 for WT and RamKO skeletal muscle, respectively. The RyR/DHPR ratio we found in WT is consistent with that found by others in total rabbit skeletal muscle homogenates and total microsomal fraction [60-62]. Assuming that there are 4 PN200-110 binding sites per tetrads and one ryanodine binding site per RyR, these results imply that in sarcotubular membranes from RamKO mice there is one tetrad-coupled RyR every 5/6 RyRs, while in WT sarcotubular membranes there is one tetrad-coupled RyR every 2-3 RyRs. The ryanodine to dihydropyridine receptor ratio of skeletal muscle from RamKO mice is more similar to that of cardiac [60] and or amphibian skeletal muscles [61] than that of mature mammalian skeletal muscle. Thus, at this time it is difficult to reconcile the functional behavior of such a large fraction of uncoupled RyR in RamKO fibers with that of uncoupled RyR presents in WT skeletal muscle having canonical ryanodine to dihydropyridine receptor ratios. Although a great deal of data do not support the notion that in mammalian skeletal muscle fibers uncoupled-RyR are activated by the calcium released from voltage sensor coupled RyRs via calcium-induced calcium release [63-65], we can not exclude the possibility that the large "cardiac-like" fraction of voltage-sensor uncoupled RyR in RamKO fibers might have distinct functional behavior.

Global calcium signals and elementary calcium release events in WT and RamKO fibres.

Measurements of global calcium in single EDL, soleus and FDB show no differences in the peak amplitude of depolarization-induced Ca^{2+} release between WT and RamKO. Such a results was unexpected because of the significant decrease of the membrane density of DHPR, and is not consistent with the general idea that the DHPR drives the voltage-dependent activation of RyR1. Nevertheless, it may be possible that the large fraction of uncoupled RyRs are sensitive to regulation by physiological modulators and the activation of the uncoupled RyRs might compensate for the lower content of voltage sensors in RamKO muscles. This line of reasoning is supported by our finding of the modification of the morphology of ECRE induced by osmotic shock, a maneuver which weakens the control of the DHPR over the RyR1, and may thus unmask a distinct regulatory mechanism of uncoupled RyR1 in RamKO fibres. ECRE in RamKO fibres are spatially wider and this does apparently not correlate with the changes of the amplitude of ECRE between WT and RamKO fibres. A larger FWHM of ECRE in FDB fibre from raptor knock-out mice may be caused by a decrease of the removal of calcium at the source site by SERCA and/or by cytosolic calcium binding proteins. A decrease of removal of calcium is likely not due to changes in the membrane density of the Ca^{2+} pump, since staining of western blots with either SERCA1 or SERCA2 Ab did not reveal differences in their protein level in crude SR membrane preparations. The wider ECRE in RamkO fibres may result from the recruitment of the larger fraction of RyRs which are not directly coupled to DHPRs, as described in frog skeletal muscles [65], a tissue with a ryanodine to dihydropyridine receptors ratio higher than that of mammalian skeletal muscle fibres [61]. If such a distinct functional behaviour is also operating in RamKO skeletal muscle fibres under physiological condition, it is possible that during an action potential voltage-operated RyR1 channels open and the calcium released by the voltage-operated RyR1s propagate to neighbouring uncoupled RyR1 channels. The latter channels release calcium by calcium-induced calcium release mechanism and ultimately contribute to the calcium transient.

Compartmentalisation of glycogen phosphorylase to SR membrane

In skeletal muscle glycogen forms a dense network of granules which are mostly localised on the myoplasmic surface of terminal cisternae and along the membrane of the fenestrated collar [66]. Excitation of skeletal muscle is associated by a rapid (seconds) glycogen breakdown via activation of glycogen phosphorylase, the enzyme responsible for the release of glucose-1-P from glycogen particles, which ultimately supports muscle metabolism during exercise. It has been demonstrated that excitation–glycolysis coupling occurs without an increase of the myoplasmic concentration of cAMP and without the subsequent conversion of GP-b to GP-a by the cAMP-dependent activity of phosphorylase kinase [67]. GP-b can be allosterically activated by AMP, this cAMP-non stimulated activity is thought to be predominant during the early phases of skeletal muscle contraction [68]. In resting conditions, the intracellular concentration of AMP is not sufficient to activate GP-b, thus GP-b is thought to be inactive in resting muscles [69]. During strenuous muscle activity however, the intracellular AMP concentration increases, signalling a demand in energy requirement. AMP is the product of the activity myokinase, an enzyme which utilises as a substrate the ADP generated by the activity of the SR CaATPase, Na-K-ATPase and myosin-ATPase. In resting conditions, the average myoplasmic concentration of AMP is 0.2 μM and it increases 10-fold during intense muscle activity [70, 71]. However, in regions of high ATP consumption such as in domains where the SERCA enzyme pumps calcium back into the SR, a greater amount ATP is required and this may be made available by the allosteric activation of GP-b by AMP. Interestingly, lower glycogen content and an increase in its degradation have been linked to a fast decay of calcium transients and force during tetanic stimulation [72, 73]. The cAMP dependent active form of GP-a inhibits the activation of the RyR1 by caffeine [48]. Thus, the presence of GP-b associated with the SR membrane is consistent with the concept that the increase in fatigue resistance described in RamKO [11] mice correlates with sustained calcium release thanks to the compartmentalisation to the SR of an energy supplying system made up of glycogen and GP-b.

Overall these results indicate that the muscle phenotype of RamKO mice is complex and due to the interaction of multiple biochemical pathways governed by the mTORC1signaling complex. This study shows that an adequate mTORC1 activity is required to maintain the structure and the function of the membrane compartments involved in excitation-contraction coupling.

Acknowledgements: We gratefully acknowledge Anne-Sylvie Monnet's technical support. This work was supported by the Department of Anesthesia, Basel University Hospital.

REFERENCES

[1]. De Virgilio, C. and Loewith, R. (2006) The TOR signalling network from yeast to man. Int. J. Biochem. Cell. Biol. **38**, 1476-1481.

[2]. Wullschleger, S., Loewith, R. and Hall, M.N. (2006) TOR signaling in growth and metabolism. Cell **124**, 471-484.

[3]. Guertin, D.A. and Sabatini, D.M. (2007) Defining the role of mTOR in cancer. Cancer. Cell. **12**, 9-22.

[4]. Yang, Q. and Guan, K.L. (2007) Expanding mTOR signaling. Cell. Res. **17**, 666-681.

[5]. Hay, N. and Sonenberg, N. (2004) Upstream and downstream of mTOR. Genes. Dev. **18**, 1926-1945.

[6]. Banaszynski, L.A., Liu, C.W. and Wandless, T.J. (2006) Characterization of the FKBP.rapamycin.FRB ternary complex. J. Am. Chem. Soc. **127**, 4715-4721.

[7]. Kim, D.H., Sarbassov, D.D., Ali, S.M., King, J.E., Latek, R.R., Erdjument-Bromage, H., Tempst, P. and Sabatini, D.M. (2002) mTOR interacts with raptor to form a nutrient-sensitive complex that signals to the cell growth machinery. Cell **110**,163-175.

[8]. Kim, D.H., Sarbassov, D.D., Ali, S.M., Latek, R.R., Guntur, K.V., Erdjument-Bromage, H., Tempst, P. and Sabatini, D.M. (2003) GbetaL, a positive regulator of the rapamycin-sensitive pathway required for the nutrient-sensitive interaction between raptor and mTOR. Mol. Cell. **11**, 895-904.

[9]. Dazert, E. and Hall, M.N. (2011) mTOR signalling in disease. Curr. Opin. Cell Biol. **23**, 705-706.

[10]. Bodine, S.C., Stitt, T.N., Gonzalez, M., Kline, W.O., Stover, G.L., Bauerlein, R., Zlotchenko, E., Scrimgeour, A., Lawrence, J.C., Glass, D.J. and Yancopoulos, G.D. (2001) Akt/mTOR pathway is a crucial regulator of skeletal muscle hypertrophy and can prevent muscle atrophy in vivo. Nat. Cell. Biol. **3**, 1009-1013.

[11]. Risson V1, Mazelin L, Roceri M, Sanchez H, Moncollin V, Corneloup C, Richard-Bulteau H, Vignaud A, Baas D, Defour A, Freyssenet D, Tanti JF, Le-Marchand-Brustel Y, Ferrier B, Conjard-Duplany A, Romanino K, Bauché S, Hantaï D, Mueller M, Kozma SC, Thomas G, Rüegg MA, Ferry A, Pende M, Bigard X, Koulmann N, Schaeffer L, Gangloff YG (2009) Muscle inactivation of mTOR causes metabolic and dystrophin defects leading to severe myopathy J. Cell Biol. **187**: 859-874

[12]. Bentzinger, C.F., Romanino, K., Cloetta, D., Lin, S., Mascarenhas, J.B., Oliveri, F., Xia, J., Casanova, E., Costa, C.F., Brink, M., Zorzato, F., Hall, M.N. and Rüegg, M.A. (2008) Skeletal muscle-specific ablation of raptor, but not of rictor, causes metabolic changes and results in muscle dystrophy. Cell. Metab. **8**, 411-424.

[13]. Rios, E. and Pizarro, G. (1991) Voltage sensor of excitation-contraction coupling in skeletal muscle. Physiol. Rev. **71**, 849-908.

[14]. Franzini-Armstrong, C. and Jorgensen, A.O. (1994) Structure and development of E-C coupling units in skeletal muscle. Annu. Rev. Physiol. **56**, 509-534.

[15]. Beam, K.G., Tanabe, T. and Numa, S. (1989) Structure, function, and regulation of the skeletal muscle dihydropyridine receptor. Ann. N. Y. Acad. Sci. **560**, 127-137.

[16]. Schneider, M.F. and Chandler, W.K. (1972) Voltage dependent charge movement of skeletal muscle: a possible step in excitation-contraction coupling. Nature **242**, 244–246.

[17]. Melzer, W., Hermann-Frank, A. and Luttgau, H.C. (1995). The role of Ca2+ ions in excitation-contraction coupling of skeletal muscle fibres. Biochim. Biophys. Acta **1241**, 59–116.

[18]. Fleischer, S. and Inui, M. (1989) Biochemistry and biophysics of excitation–contraction coupling. Annu. Rev. Biophys. Biophys. Chem. **18**, 333–364.
[19]. Treves, S., Jungbluth, H., Muntoni, F. and Zorzato, F. (2008) Congenital muscle disorders with cores: the ryanodine receptor calcium channel paradigm. Curr. Opin. Pharmacol. **8**, 319-326.
[20]. Anderson, A.A., Treves, S., Biral, D., Betto, R., Sandonà, D., Ronjat, M. and Zorzato, F. (2003) The novel skeletal muscle sarcoplasmic reticulum JP-45 protein: molecular cloning, tissue distribution, developmental expression and interaction with α.1 subunit of the voltage gated calcium channel. J. Biol.Chem. **278**: 39987-39992.
[21]. Saito, A., Seiler, S. Chu, A. and Fleischer, S. (1984) Preparation and morphology of sarcoplasmic reticulum terminal cisternae from rabbit skeletal muscle. J. Cell. Biol. **99**, 875-885.
[22]. Treves, S., Thurnheer, R., Mosca, B., Vukcevic, M., Bergamelli, L., Voltan, R., Oberhauser, V., Ronjat, M., Csernoch, L., Szentesi, P. and Zorzato, F. (2012) SRP-35, a newly identified protein of the skeletal muscle sarcoplasmic reticulum, is a retinol dehydrogenase. Biochem. J. **44**, 731-741.
[23]. Delbono, O., Xia, J., Treves, S., Wang, Z.M., Jimenez-Moreno, R., Payne, A.M., Messi, M.L., Briguet, A., Schaerer, F., Nishi, M., Takeshima, H. and Zorzato, F. (2007) Loss of skeletal muscle strength by ablation of the sarcoplasmic reticulum protein JP45. Proc. Natl. Acad. Sci. U.S.A. **104**, 20108-20113.
[24]. Fabiato, A. (1988) Computer programs for calculating total from specified free or free from specified total ionic concentrations in aqueous solutions containing multiple metals and ligands. Methods. Enzymol. **157**, 378-417.
[25]. Calderon, J.C., Bolanos, P. and Caputo, C. (2010) Myosin heavy chain isoform composition and Ca2+ transients in fibres from enzymatically dissociated murine soleus and extensor digitorum longus muscles. J. Physiol. **588**, 267-279.
[26]. Wang, X., Weisleder, N., Collet, C., Zhou, J., Chu, Y., Hirata, Y., Zhao, X., Pan, Z., Brotto, M., Cheng, H. and Ma, J. (2005) Uncontrolled calcium sparks act as a dystrophic signal for mammalian skeletal muscle. Nat Cell Biol. **7**, 525-530.
[27]. Apostol, S., Ursu, D., Lehmann-Horn, F. and Melzer, W. (2009) Local calcium signals induced by hyper-osmotic stress in mammalian skeletal muscle cells. J. Muscle Res. Cell. Motil. **30**, 97–109.
[28]. Schindelin J., Arganda-Carreras, I., Frise, E., Kaynig, V., Longair, M., Pietzsch, T., Preibisch, S., Rueden, C., Saalfeld, S., Schmid, B., Tinevez, J.Y., White, D.J., Hartenstein, V., Eliceiri, K., Tomancak, P. and Cardona, A. (2001) Fiji: an open-source platform for biological-image analysis. Nature Methods **9**, 676-682.
[29]. Picht, E., Zima, A.V., Blatter, L.A. and Bers, D.M. 2007. SparkMaster: automated calcium spark analysis with ImageJ. Am. J. Physiol. Cell. Physiol**. 293**, C1073-C1081.
[30]. Kirsch, W.G., Uttenweiler, D. and Fink, R.H. (2001) Spark- and ember-like elementary Ca2+ release events in skinned fibres of adult mammalian skeletal muscle. J. Physiol. **537**, 379-89
[31]. Hollingworth, S., Peet, J., Chandler, W.K. and Baylor, S.M. (2001) Calcium sparks in intact skeletal muscle fibers of the frog. J Gen Physiol. **118**, 653-678.
[32]. Danforth, W.H., Helmreich, E. and Coric, F. (1962) The effect of contraction and of epinephrine on the phosphorylase activity of frog sartorius muscle. Proc. Natl. Acad. Sci. U.S.A. **48**, 1191-1199.
[33]. Chasiotis, D., Brandt, R., Harris, R.C. and Hultman, E. (1983) Effects of beta-blockade on glycogen metabolism in human subjects during exercise. Am. J. Physiol. **245**, E166-170.

[34]. Rush, J.W. and Spriet, L.L. (2001). Skeletal muscle glycogen phosphorylase a kinetics: effects of adenine nucleotides and caffeine. J. Appl. Physiol. **91**, 2071-2078.
[35]. Zheng, Z., Wang, Z.M. and Delbono, O. (2002) Charge movement and transcription regulation of L-type calcium channel alpha(1S) in skeletal muscle cells. J. Physiol. **540**, 397-409.
[36]. Lamb, G.D. and Stephenson, D.G. (1996) Effects of FK506 and rapamycin on excitation-contraction coupling in skeletal muscle fibres of the rat. J. Physiol. **494**,569-576.
[37]. Avila, G. and Dirksen, R.T. (2005) Rapamycin and FK506 reduce skeletal muscle voltage sensor expression and function. Cell Calcium **38**, 35-44.
[38]. Yoshida, M., Minamisawa, S., Shimura, M., Komazak, S., Kume, H., Zhang, M., Matsumura, K., Nishi, M., Saito, M., Saeki, Y., Ishikawa, Y., Yanagisawa, T. and Takeshima, H. (2005) Impaired Ca^{2+} store functions in skeletal and cardiac muscle from sarcalumenin-deficient mice. J. Biol. Chem. **280**, 3500-3506.
[39]. Knudson, C.M. and Campbell, K.P. (1989) Albumin is a major protein component of transverse tubule vesicles isolated from skeletal muscle. J. Biol. Chem. **264**, 10795-10798.
[40]. Peng, T., Golub, T.R. and Sabatini, D.M. (2002) The immunosuppressant rapamycin mimics a starvation-like signal distinct from amino acid and glucose deprivation. Mol. Cell. Biol. **22**, 5575-5584.
[41]. Shin, D.W., Pan, Z., Bandyopadhyay, A., Bhat, M.B., Kim, D.H., Ma, J. (2002) Ca2+-dependent interaction between FKBP12 and calcineurin regulates activity of the Ca2+ release channel in skeletal muscle Biophys J. **83**: 2539-25492.
[42]. Nyfeler, B., Bergman, P., Triantafellow, E., Wilson, C.J., Zhu ,Y., Radetich, B., Finan, P.M., Klionsky, D.J., Murphy, L.O. (2011) Relieving autophagy and 4EBP1 from rapamycin resistance Mol Cell Biol **31**: 2867-2876.
[43]. Andersson, D.C., Betzenhauser, M.J., Reiken, S., Meli, A.C., Umanskaya, A., Xie, W., Shiomi, T., Zalk, R., Lacampagne, A., Marks, A.R. (2011) Ryanodine receptor oxidation causes intracellular calcium leak and muscle weakness in aging Cell Metab. **14**:196-207
[44]. Durham WJ, Aracena-Parks P, Long C, Rossi AE, Goonasekera SA, Boncompagni S, Galvan DL, Gilman CP, Baker MR, Shirokova N, Protasi F, Dirksen R, Hamilton SL. (2008) RyR1 S-nitrosylation underlies environmental heat stroke and sudden death in Y522S RyR1 knockin mice Cell. **133**:53-65.
[45]. Cuenda, A., Henao, F., Nogues, M. and Gutierrez-Merino, C. (1994) Quantification and removal of glycogen phosphorylase and other enzymes associated with sarcoplasmic reticulum membrane preparations. Biochim. Biophys. Acta. **1194**, 35-43.
[46]. Johnson LN (1992) Glycogen phosphorylase: control by phosphorylation and allosteric effectors. FASEB J. **6**, 2274–2282.
[47]. Cuenda, A., Nogues, M., Henao, F. and Gutierrez-Merino, C. (1995). Interaction between glycogen phosphorylase and sarcoplasmic reticulum membranes and its functional implications. J. Biol. Chem. **270**, 11998-12004.
[48]. Hirata Y., Atsumi, M., Ohizumi, Y. and Nakahata, N. (2003) Mastoparan binds to glycogen phosphorylase to regulate sarcoplsmic reticulm Ca2+ release in skeletal muscle. Biochem. J. **371**, 81-88.
[49]. Hollingworth, S., Gee, K.R. and Baylor, S.M. (2009) Low-affinity Ca2+ indicators compared in measurements of skeletal muscle Ca2+ transients. Biophys J. **97**, 1864-1872.

[50]. Heizmann, C.W., Berchtold, M.W., Rowlerson, A.M. (1982) Correlation of parvalbumin concentration with relaxation speed in mammalian muscles. Proc. Natl. Acad. Sci. **79**: 7243-7247

[51]. Baylor, S.M., Hollingworth. S. (2012) Intracellular calcium movements during excitation-contraction coupling in mammalian slow-twitch and fast-twitch muscle fibers.J. Gen. Physiol. **13** :261–272

[52]. Zhou, J., Yi, J., Royer, L., Launikonis, B.S., Gonzalez, A., Garcia, J. and Rios, E. (2006) A probably role of dihydropyridine receptors in repression of Ca^{2+} sparks demonstrated in cultured mammalian muscle. Am. J. Physiol Cell Physiol. **290**, C539-C553.

[53]. Jung, C.H., Ro, S.H., Cao, J., Otto, N.M. and Kim, D.H. (2010) mTOR regulation of autophagy. FEBS Lett. **584**, 1287-1295.

[54]. Harston, R.K., McKillop, J.C., Moschella, P.C., Van Laer, A., Quinones, L.S., Baicu, C.F., Balasubramanian S., Zile, M.R. and Kuppuswamy, D. (2011) Rapamycin treatment augments both protein ubiquitination and Akt activation in pressure -overloaded rat myocardium. Am. J. Physiol. Heart Circ. Physiol. **300**, H1696-H1706.

[55]. Delbono, O. and Meissner, G. (1996) Sarcoplasmic reticulum Ca2+ release in rat slow and fast-twitch muscles. J. Membr. Biol. **151**, 123-130.

[56]. Zhou, H., Lillis, S., Loy, R.E., Ghassemi, F., Rose, M.R., Norwood, F., Mills, K., Al-Sarraj, S., Lane, R.J., Feng, L., Matthews, E., Sewry, C.A., Abbs, S., Buk, S., Hanna, M., Treves, S., Dirksen, R.T., Meissner, G., Muntoni, F. and Jungbluth, H. (2010) Multi-minicore Disease and atypical periodic paralysis associated with novel mutations in the skeletal muscle ryanodine receptor (RYR1) gene. Neuromuscul. Disord. **20**,166-173.

[57]. Al-Qusairi, L., Weiss, N., Toussaint, A., Berbey, C., Messaddeq, N., Kretz, C., Sanoudou, D., Beggs, A.H., Allard, B., Mandel, J.L., Laporte, J., Jacquemond, V. and Buj-Bello, A. (2009) T-tubule disorganization and defective excitation-contraction coupling in muscle fibers lacking myotubularin lipid phosphatase. Proc. Natl. Acad. Sci. U.S.A. **106**,18763-18768.

[58]. Bevilacqua, J.A., Bitoun, M., Biancalana, V., Oldfors, A., Stoltenburg, G., Claeys, K.G., Lacène, E., Brochier, G., Manéré, L., Laforêt, P., Eymard, B., Guicheney, P., Fardeau, M. and Romero, N.B. (2009) Neclace fibers, a new histological marker of late onset MTM1-related centronuclear myopathy. Acta Neuropathol. **117**, 283-291

[59]. Razidlo, G.L., Katafiasz, D. and Taylor, G.S. (2011) Myotubularin regulates Akt-dependent survival signaling via phosphatidylinositol 3-phosphate. J. Biol. Chem. **286**, 20005-20019.

[60]. Bers, D.M. and Stiffel., V.M. (1993) Ratio of ryanodine to dihydropyridine receptors in cardiac and skeletal muscle and implications for E-C coupling. Am. J. Physiol. **264**, C1587-C1593.

[61]. Anderson, K., Cohn, A.H. and Meissner, G. (1994) High-affinity [3H]PN200-110 and [3H]ryanodine binding to rabbit and frog skeletal muscle. Am J Physiol. **266**, C462-C466.

[62]. Margreth, A., Damiani, E. and Tobaldin, G. (1993) Ratio of dihydropyridine to ryanodine receptors in mammalian and frog twitch muscles in relation to the mechanical hypothesis of excitation-contraction coupling. Biochem. Biophys. Res. Commun. **197**, 1303-11.

[63]. Shirokova, N., Garcia, J. and Rios, E. (1998) Local Ca^{2+} release in mammalian skeletal muscle. J. Physiol. **512,** 377-384.

[64]. Figueroa, L., Shkryl, V.M., Zhou, J., Manno, C., Marmotake, A., Brum, G., Blatter, L.A., Elli-Davies, G.C. and Rios, E. (2012) Synthetic localized calcium transients directly probe signalling mechanisms in skeletal muscle. J. Physiol. **590**, 1389-1411.
[65]. González, A., Kirsch,W.G., Shirokova, N., Pizarro G., Stern, M.D. and Ríos, E. (2000) The spark and its ember: separately gated local components of Ca^{2+} release in skeletal muscle J Gen Physiol. **115**,139-58.
[66]. Peachey, L.D. (1965) The sarcoplasmic reticulum and transverse tubules of the frog's sartorius J. Cell Biol. **25**, 209-231.
[67]. Drummond, G. I., Hanvood, J. P. and Powell, C. A. (1969) Studies on the activation of phosphorylase in skeletal muscle by contraction and by epinephrine J. Biol. Chem. **244**, 4235-4240.
[68]. Entman, M.L., Keslensk,y S..S, Chu, A. and Van Winkle, W.B. (1980) The sarcoplasmic reticulum-glycogenolytic complex in mammalian fast twitch skeletal muscle. Proposed in vitro counterpart of the contraction-activated glycogenolytic pool. J. Biol. Chem. **255**, 6245-6252.
[69]. Katz, A., Andersson, D.C., Yu, J., Norman, B., Sandstrom, M.E., Wieringa, B. and Westerblad, H. (2003) Contraction-mediated glycogenolysis in mouse skeletal muscle lacking creatine kinase: the role of phosphorylase b activation. J. Physiol. **553**, 523-531.
[70]. Hellstein, Y., Richter, E.A., Kiens, B. and Bangsbo, J. (1999) AMP deamination and purine exchange in human skeletal muscle during and after intense exercise. J. Physiol. **520**, 909-920.
[71]. Allen, D.G., Lamb, G.D. and Westerblad, H. (2007). Impaired calcium release during fatigue. J. Appl. Physiol. **104**, 296-305.
[72]. Stephenson, D.G. (2011) In pursuit of the glycogen [Ca2+] connection. J. Physiol **589**, 451.
[73]. Ortenblad, N., Nielsen, J., Saltin, B. and Holmberg, H.C. (2011) Role of glycogen availability in sarcoplasmic reticulum Ca2+ kinetics in human skeletal muscle. J. Physiol **589**, 711-725.

Table 1
Kinetic properties of calcium transients of isolated EDL and soleus fibers from control and RamKO mice

	Resting Ca^{2+} [nM] [a]	Peak Amplitude[b] ΔF/F	Time to peak (ms)	Rise Time 10-90% (ms)	Fall Time 10-90% (ms)
EDL control	141.0±0.35 (n=23)	0.46±0.04 (n=29)	2.9±0.1 (n=29)	1.7±0.05 (n=29)	34.1±4.3 (n=29)
EDL RAmKO	115.5±4.8* (n=21)	0.43±0.02 (n=27)	3±0.1 (n=27)	1.8±0.06 (n=27)	39.4±5.4 (n=27)
Soleus control	117±3.6 (n=26)	0.38±0.02 (n=22)	3.4±0.2 (n=22)	2.1±0.2 (n=22)	66.2±7.4 (n=22)
Soleus RAmKO	93.8±4.26* (n=8)	0.36±0.02 (n=25)	3.4±0.1 (n=25)	2.1±0.1 (n=25)	120.3±15.7* (n=25)

Values are mean+/-s.e.m., n= number of fibres from 6 WT and RamKO mice
*P<0.05 Mann Whitney U test,
[a] Calcium measurements performed with the ratiometric indicator indo-1;
[b] Calcium measurements performed with Mag-Fluo-4;

Table 2

Morphology of ECREs in Skeletal muscle fibers

		Amplitude ($\Delta F/F_0$)	FWHM (μm)	FDHM (ms)	Mass	Freq[a] (Sparks/image)	N[b]
<50 ms ECREs	WT	0.38±0.00	0.89±0.01	13.31±0.26	0.62±0.02	6.81±0.36	1923
	RamKO	0.38±0.00	0.98±0.01*	14.11±0.24*	0.85±0.03*	8.83±0.40*	2547
>50 ms ECREs	WT	0.56±0.01	1.32±0.02	143.36±3.32	2.51±0.17	2.51±0.17	538
	RamKO	0.60±0.01*	1.45±0.02*	138.49±2.80	3.56±0.18*	3.56±0.18*	731

Values are expressed as mean ± s.e.m..
[a]: WT 168 images, RamKO 162 images
[b]: number of ECREs analyzed in 25 fibres and 26 fibres from 5 WT and RamKO 5 mice, respctively.

Figure legends:

Figure 1: Mechanical properties of isolated EDL and soleus muscles from RamKO and control littermates. Isolated muscles from 8 week-old mice were electrically stimulated as described in the Experimental Procedures section. Top panels show single twitches, bottom panels maximal tetanus force. Dotted line RamKO mice, continuous line control littermates. Note that the muscles from RamKO mice developed approximately 20% less force than controls. Slow twitch muscles also showed a significant decrease in the half relaxation time. Traces are representative of experiments carried out by Bentzinger et al. [12] on at least 3/4 different muscle preparations.

Figure 2: **Biochemical characterization of SR proteins from RamKO mice**. Left panels show representative Western blots with specified antibodies; right panels, mean band intensity (±SD) of 6-9 determinations from 3 different SR preparations. Values were normalized with respect to intensity values obtained from control littermates. White bars, controls; black bars, RamKO. **P<0.002.

Figure 3: $Ca_v1.1$ is decreased in RamKO mice. **A.** Equilibrium binding of PN200-110 to skeletal muscle SR of control (filled circle) and RamKO (empty boxes) mice. Data points represent mean (± S.E.M.) of 6 determinations carried out in two different SR preparations. **B.** and **C.** Western blots of Ca_V 1.1 and Ca_V β1 in SR of control (empty bars) and RamKO mice (filled bars) and mean band of 5-7 determinations from 3 different SR preparations.

Figure 4: $Ca_v1.1$ decrease in RamKO mice is not due to a decrease in transcription of $Ca_v1.1$ mRNA. A. Semi-quantitative RT-PCR of $Ca_v1.1$. The figure represents results obtained in four different experiments with RNA extracted from two muscle preparations. **B.** Western blot of total muscle homogenate with anti-$Ca_v1.1$ and anti-albumin, a marker for transverse tubule content. The bar histogram shows mean (±S.E.M.) band intensity of 6 determinations from 4 different muscle preparation; band intensity from the RamKO mice are normalized to that obtained in control littermates. **C.** The $Ca_v1.1$ promoter is not affected by treatment with 20 μM rapamycin as determined by luciferase activity. No activity was seen upon transfection of cells with a control plasmid (white bars) nor upon transfection of HEK293 with the luciferase reporter (black bars). C_2C_{12} cells transfected with a control plasmid showed no luciferase activity, while transfection with the luciferase reporter resulted in strong activity which was not affected by 2 or 16 h incubation with rapamycin (black bars). **D.** Rapamycin treatment of C_2C_{12} cells was effective as it resulted in the decrease of phosphorylation of S6 after 2 and 16 hours. **E.** Rapamycin treatment of differentiated C_2C_{12} causes a decrease in $Ca_V1.1$ as determined by Western blotting. Cells were treated with 20 μM rapamycin for 16 hours and 25 μg of microsomes were loaded on a 7.5% SDS PAG and blotted onto nitrocellulose. Blot was probed with anti - $Ca_V1.1$, stripped and re-probed with anti-calreticulin Ab as a loading control. Asterisk indicates the band corresponding to the $Ca_V1.1$ protein.

Figure 5: Ryanodine receptor content and functional characteristics are not changed in RamKO mice. Left panel- Representative Western blot of total SR and mean band intensities (±SD) of 8 determinations from 3 different SR preparations. Top Right-[^{3}H]Ryanodine binding to SR preparations from control (filled circles) and RamKO (open boxes) mice were performed as described in the Experimental Procedures. Data points represent the mean (±S.E.M.) of 12 determinations from 3 different SR preparations. No significant change in the B_{max} or apparent K_D was found. Bottom Right- Ca^{2+} dependent [^{3}H]Ryanodine binding to SR preparations from control (filled circles) and RamKO (open boxes) mice. Data points represent mean (±S.E.M.) of 6 determinations on 2 different SR preparations.

Figure 6: Glycogen Phosphorylase (GP) is accumulated in the SR of RamKO mice and represents mainly the enzymatically inactive form. (A) Ten μg of protein from total skeletal muscle homogenate, myoplasm or SR fraction was separated on a 7.5% SDS-PAGE and stained with SimplyBlue Safe Stain. **(B)** Densitometric analysis of GP band in total SR of

control (white bars) and RamKO (black bar) mice. **(C)** SR was fractioned into light SR (R1), longitudinal SR (R2) and terminal cisternae (R4). Fifteen μg of protein from each fraction was loaded on a 7.5% SDS-PAGE and stained with SimplyBlue Safe Stain or **(D)** blotted onto nitrocellulose and stained with anti-glycogen phosphorylase Abs. White arrows in C indicate glycogen phosphorylase, which is enriched in the light SR fraction R1. **(E)** Total (left bar histogram) and inactive form (right bar histogram) glycogen phosphorylase enzymatic activity in SR from control (white bars) and RamKO (black bars) mice. Values represent the mean (± S.D.) of 11 determinations from 3 different SR preparations. *** $P<0.05$

Figure 7: Changes in the myoplasmic [Ca^{2+}] of individual, chemically dissected EDL and soleus fibres. Control and RamKO fibres were loaded with 10 μM Mag-Fluo-4AM in Tyrode's Solution for 10-15 minutes at 20°C. This solution was replaced and acquisitions were made during continuous perfusion with Tyrode's buffer plus 50 μM BTS. Calcium transients were elicited by single pulses of 1 ms duration, through a platinum electrode inside a glass pipette placed near the fibre surface. The representative traces from EDL (panel A) and soleus (panel B) show no differences in the peaks and velocities of the Ca^{2+} transients; there is a significant increase in the half relaxation time in soleus fibres from RamKO mice. See Table I for a thorough analysis of the kinetic parameters.

Figure 8: Osmotic-shock triggered ECRE are more frequent in FBD fibres from RamKO than WT mice. ECREs were triggered by exposure of FDB fibres to a hyperosmotic solution. Panels A-F: left images show Fluo4 fluorescence and right images brightfield images of the same FDB fibre. Scale bar = 30 μm. Panels **A** and **D** show (*xy*) images of the calcium fluorescence (AU) in WT and RamKO fibres in Normal Ringer, panels **B** and **E** show images of the same fibres after hyperosmotic shock treatment and **C** and **F** show images of the fibres after 10 min re-perfusion with a normo-osmotic Ringer solution; as shown after removal of the hyperosmotic medium ECRE are no longer visible. Panels **H** and **I** are pseudocoloured linescan images (*xt*) showing in detail the ECREs shape in WT an RamKO fibres when bathed with hypertonic solution. Panels **J** and **K** show that ECREs are due to the openining of RyRs as they are abolished by a 30 min pre- incubation with 10 μM. Scale bar panels H-K: Horizontal: 100 ms, Vertical: 10 μm.

Figure 1

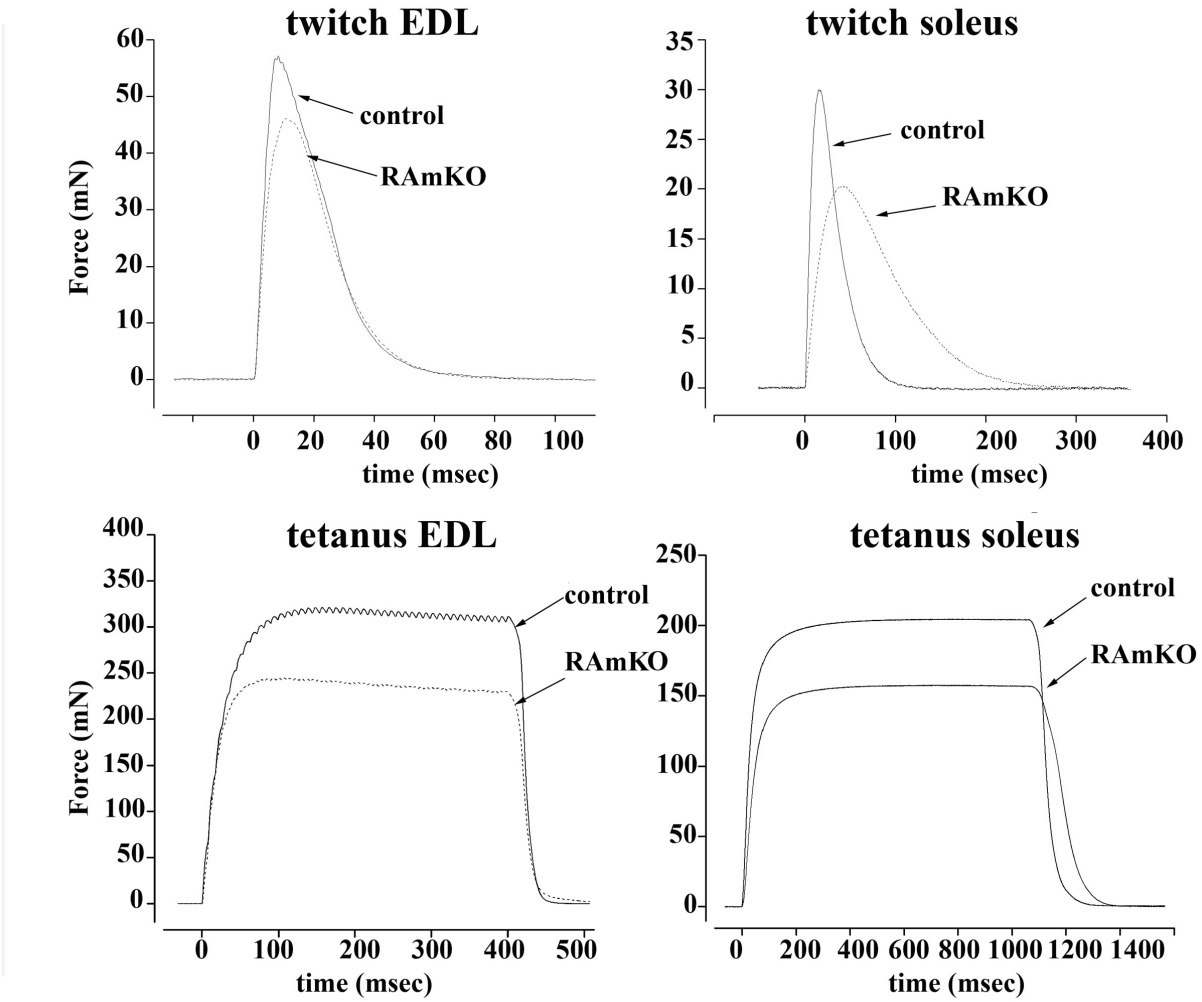
twitch EDL
control
RAmKO
Force (mN)
time (msec)
twitch soleus
control
RAmKO
time (msec)
tetanus EDL
control
RAmKO
Force (mN)
time (msec)
tetanus soleus
control
RAmKO
time (msec)

Figure 2

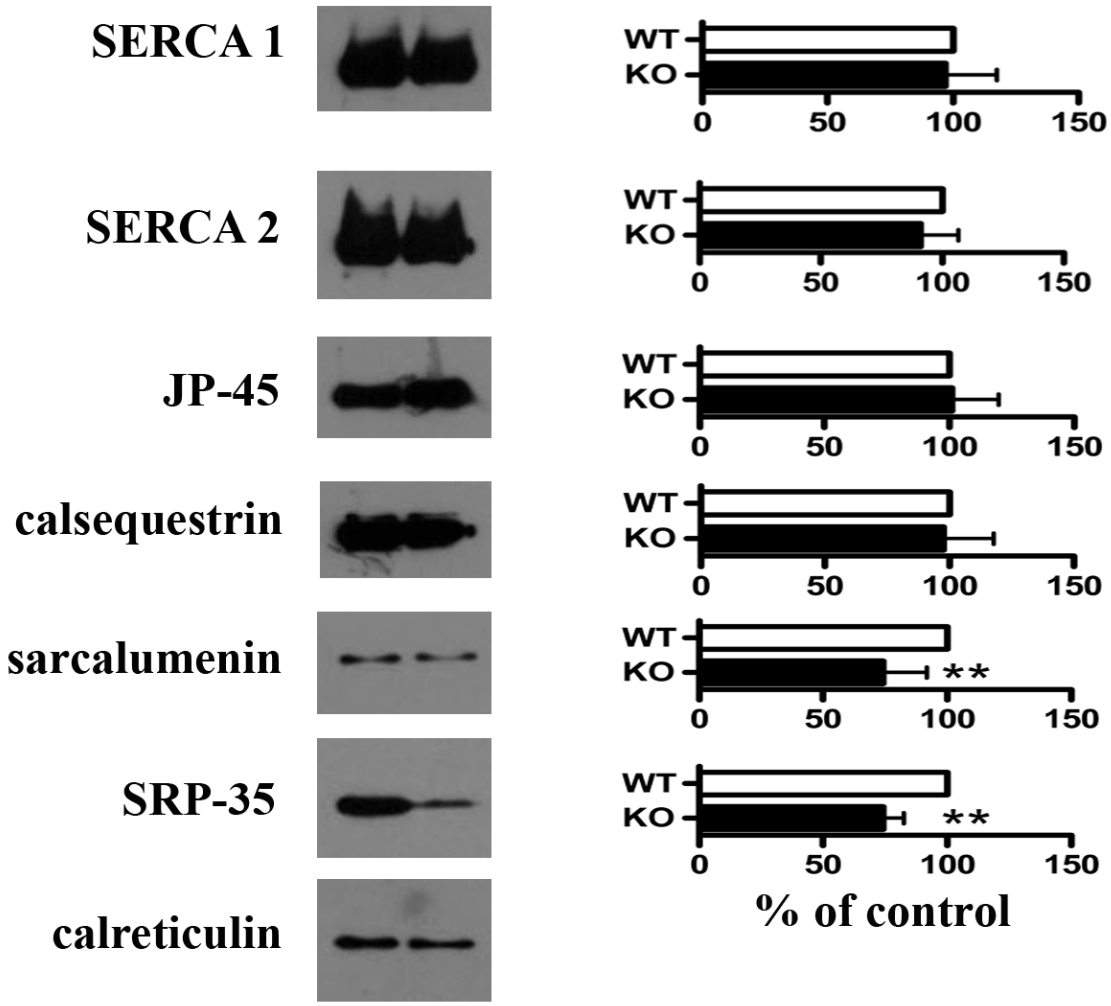
SERCA 1
SERCA 2
JP-45
calsequestrin
sarcalumenin
SRP-35
calreticulin
WT
KO
0
50
100
150
**
**
% of control

Figure 3

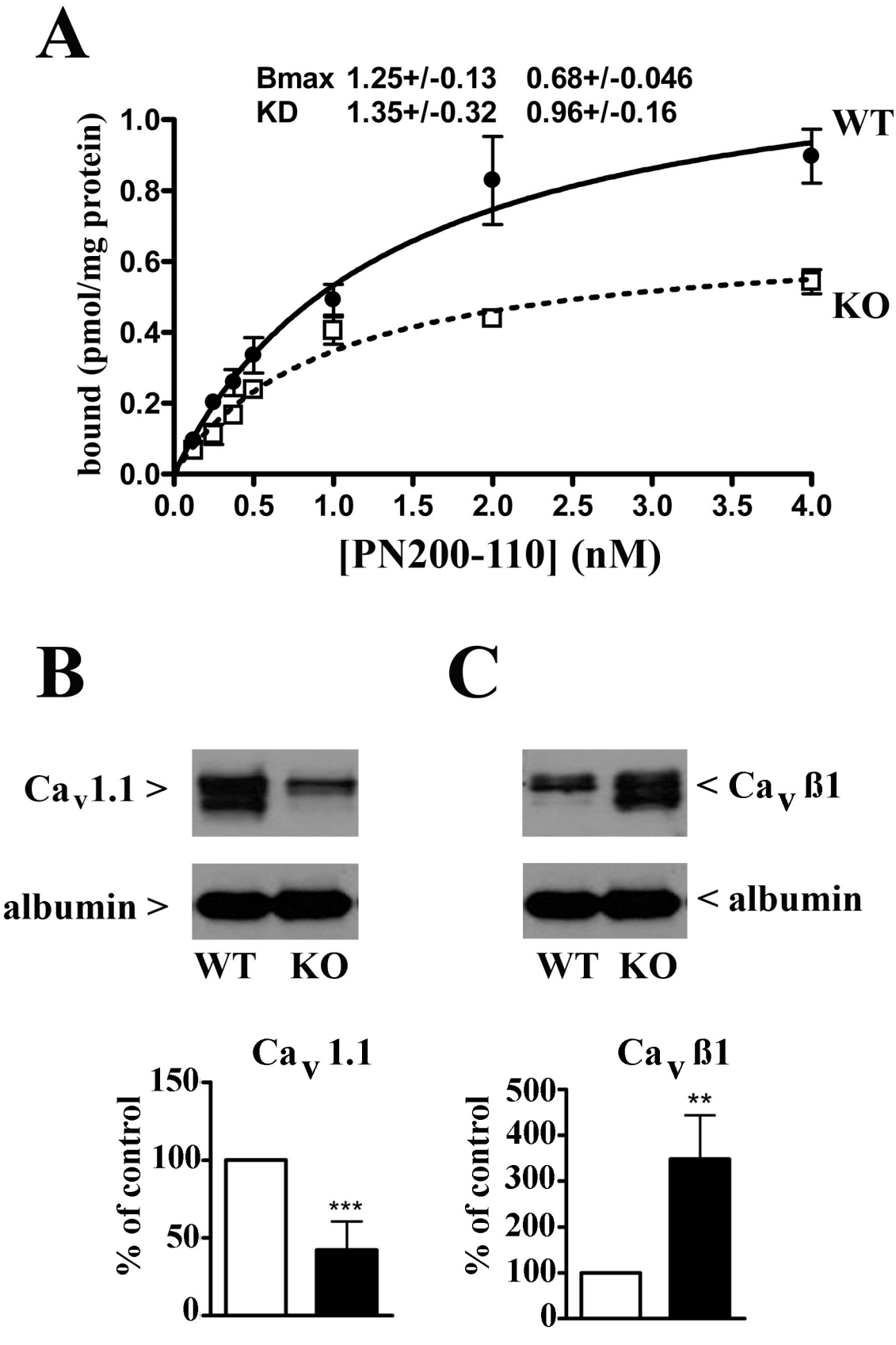
A
Bmax 1.25+/-0.13 0.68+/-0.046
KD 1.35+/-0.32 0.96+/-0.16
WT
KO
bound (pmol/mg protein)
[PN200-110] (nM)
B
C
Ca$_V$1.1 >
albumin >
WT KO
< Ca$_V$ß1
< albumin
WT KO
Ca$_V$ 1.1
% of control
***
Ca$_V$ß1
% of control
**

Figure 4

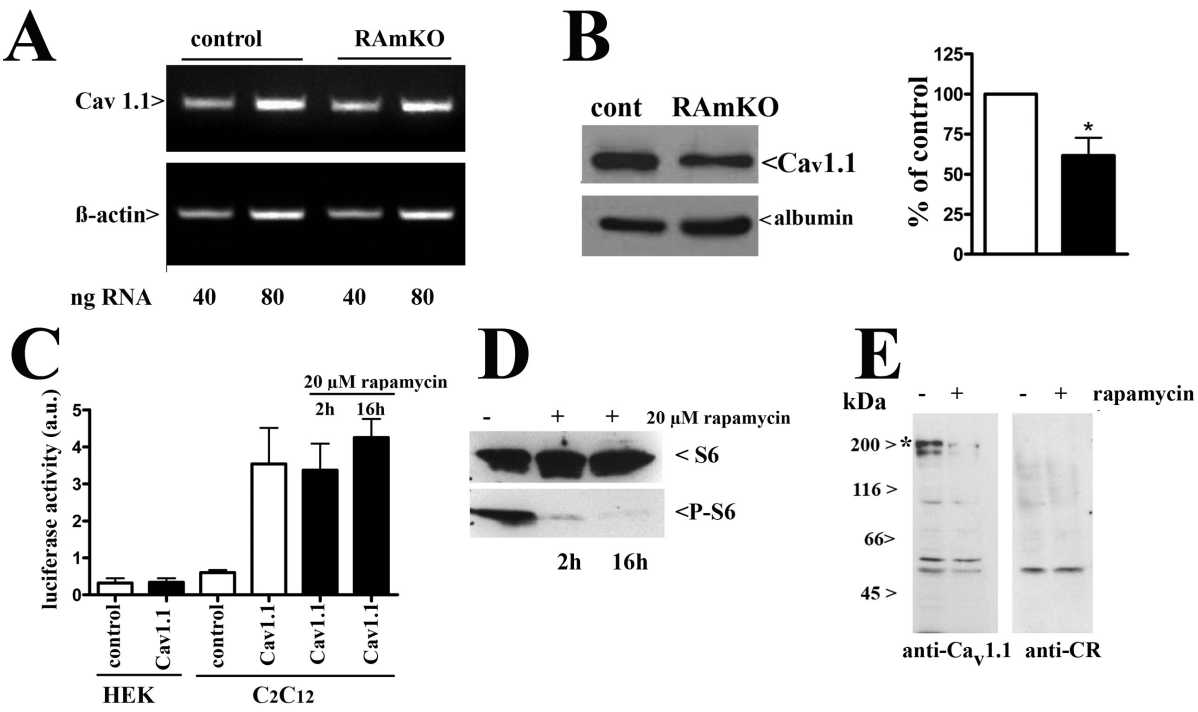
A
control
RAmKO
Cav 1.1>
ß-actin>
ng RNA 40 80 40 80
B
cont RAmKO
<Cav1.1
<albumin
% of control
125
100
75
50
25
0
*
C
20 µM rapamycin
2h 16h
luciferase activity (a.u.)
5
4
3
2
1
0
control
Cav1.1
control
Cav1.1
Cav1.1
Cav1.1
HEK
C2C12
D
- + + 20 µM rapamycin
< S6
<P-S6
2h 16h
E
kDa
- + - + rapamycin
200 > *
116 >
66>
45 >
anti-Cav1.1
anti-CR

Figure 5

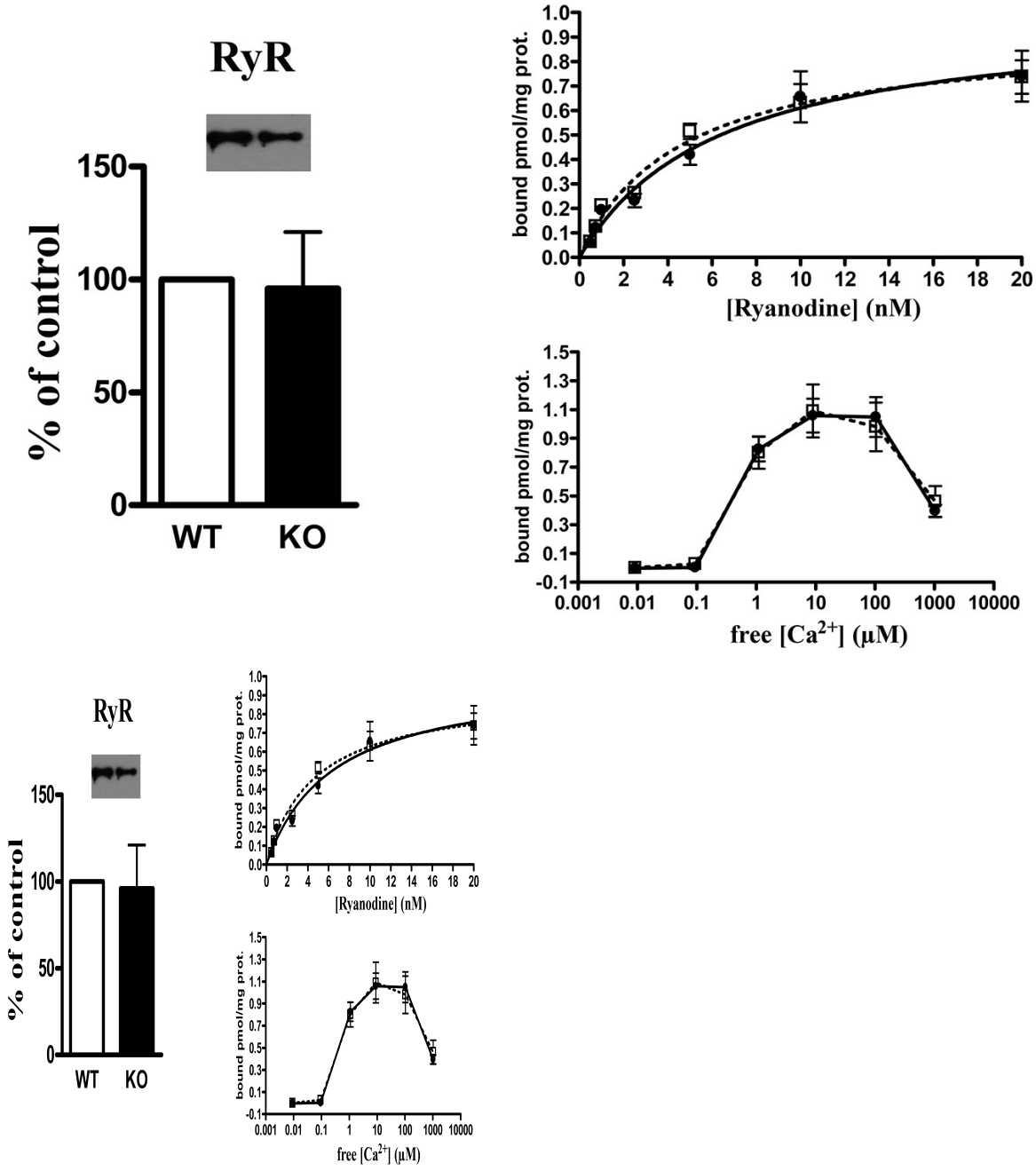
RyR
% of control
150
100
50
0
WT
KO
bound pmol/mg prot.
[Ryanodine] (nM)
free [Ca2+] (µM)

Figure 6

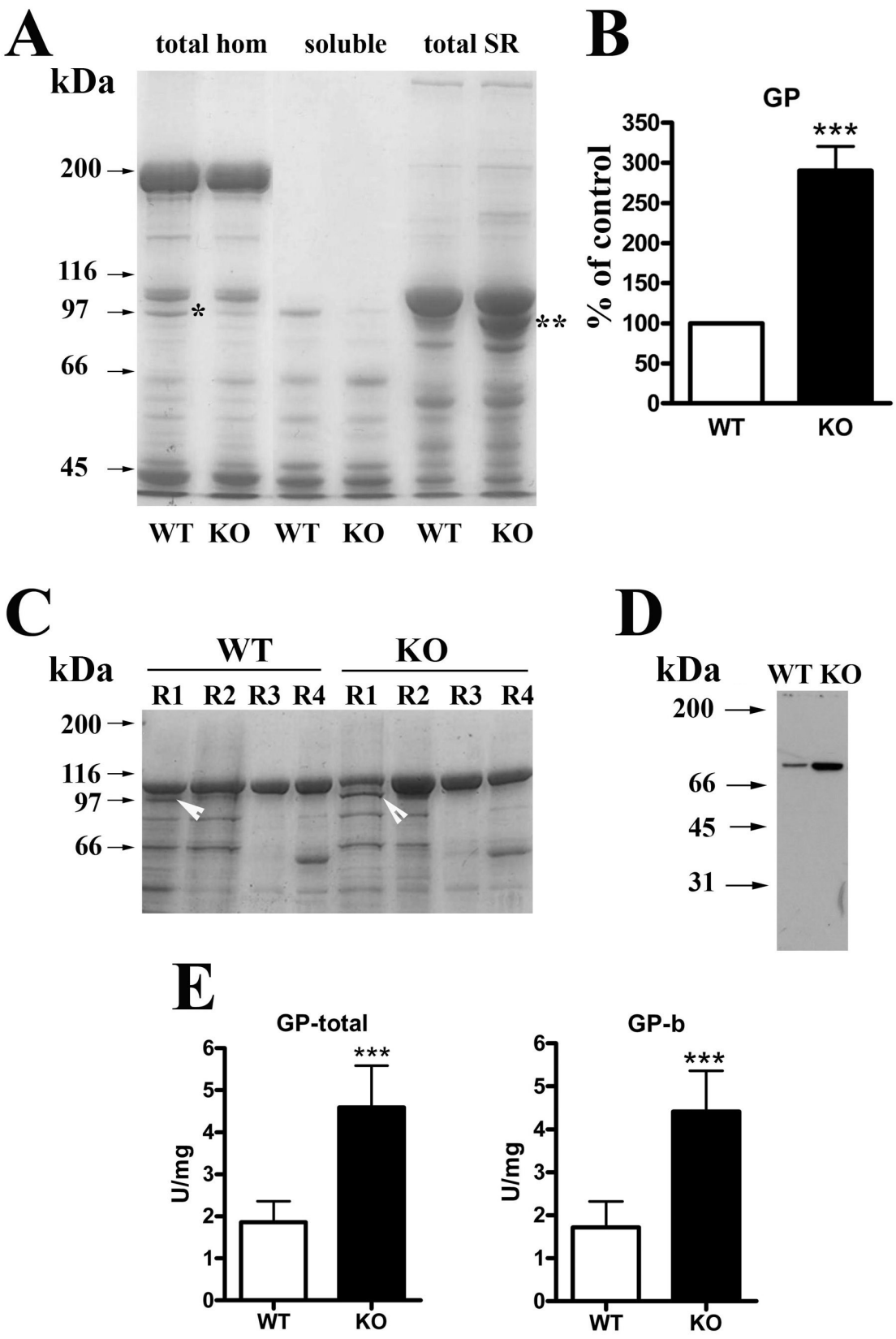
A
total hom
soluble
total SR
kDa
200
116
97
66
45
*
**
WT KO WT KO WT KO
B
GP
% of control
350
300
250
200
150
100
50
0
***
WT
KO
C
kDa
WT
KO
R1 R2 R3 R4 R1 R2 R3 R4
200
116
97
66
D
kDa
WT KO
200
66
45
31
E
GP-total
U/mg
6
5
4
3
2
1
0
***
WT
KO
GP-b
U/mg
6
5
4
3
2
1
0
***
WT
KO

Figure 7

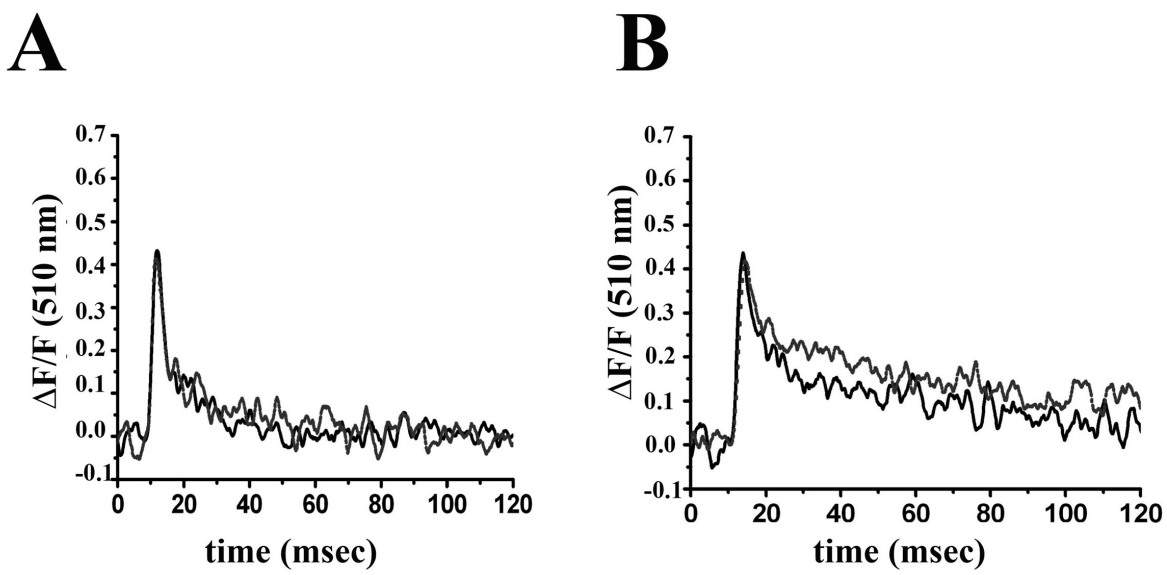
A
B
ΔF/F (510 nm)
time (msec)
0.7
0.6
0.5
0.4
0.3
0.2
0.1
0.0
-0.1
0
20
40
60
80
100
120

Figure 8

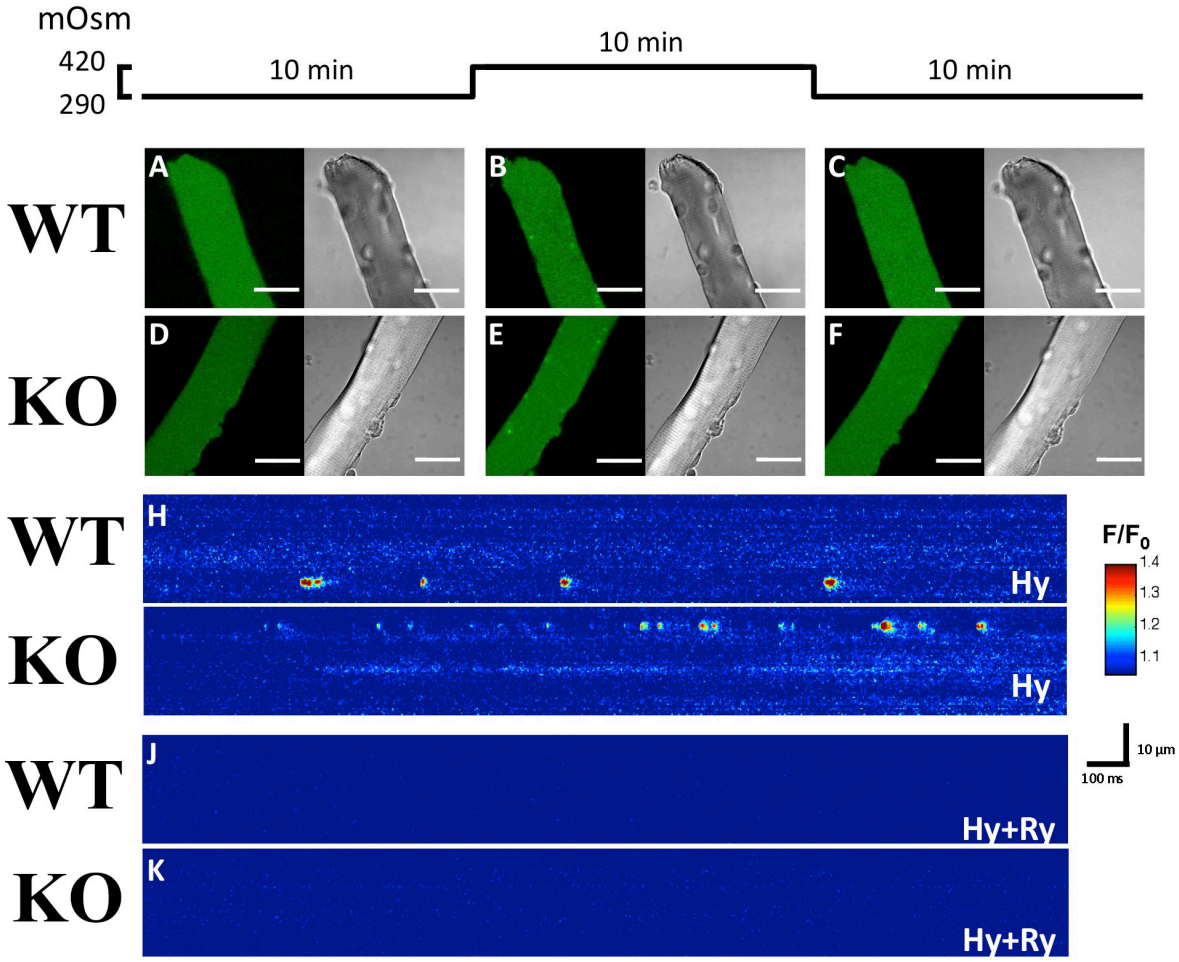
mOsm
420
290
10 min
10 min
10 min
WT
KO
A
B
C
D
E
F
WT
KO
H
Hy
Hy
F/F0
1.4
1.3
1.2
1.1
10 µm
100 ms
WT
KO
J
Hy+Ry
K
Hy+Ry

15. Supplementary figures

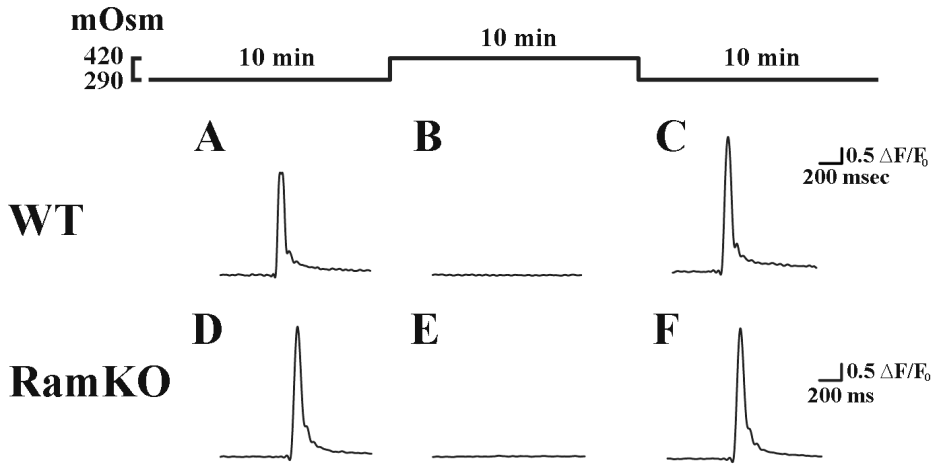

Supplementary Figure 1. Global Ca^{2+} transients in mouse FDB fibers isolated from WT and RamKO littermates elicited before and after hyperosmotic stress-induced-ECREs. FDB fibers were loaded with Fluo4 and electrically stimulated to check their viability before, during and after application of the hypertonic solution. Panels A and D display representative traces of Ca^{2+} transient triggered by an electrical pulse (4ms, 30-40 V) in WT (panel A) and RamKO (panel B) fibers respectively. Cells lose the ability to contract after a 10 min exposure to the hyperosmotic solution (B, E). Panels C and F show that the Ca^{2+} transients recover after 10 min of washing with NR (290 mOsm).